JPET Fast Forward. Published on April 9, 2004 as DOI: 10.1124/jpet.104.066175

INTRA-TUMORAL NAMI-A TREATMENT TRIGGERS METASTASIS REDUCTION, WHICH CORRELATES TO CD44 REGULATION AND TIL RECRUITMENT*

Sabrina Pacor ✉ [1], Sonia Zorzet[1], Moreno Cocchietto[2], Marina Bacac[1], Marta Vadori[1], Claudia Turrin[2], Barbara Gava[1], Anna Castellarin[2] and Gianni Sava[1,2].

[1] Department of Biomedical Sciences, University of Trieste, Trieste, ITALY

[2] Callerio Foundation-Onlus, Institutes of Biological Research, Trieste, ITALY

Running title:

REDUCTION OF MALIGNANCY BY NAMI-A

Keywords:

CD44, metastases, local chemotherapy

✉ Correspondence and address for offprint: Sabrina Pacor, Department of Biomedical Sciences, University of Trieste, via L. Giorgieri 7-9, 34127 Trieste, Italy. Phone: +39-40-558-3529; Fax +39-40-577435; E-mail: pacorsab@univ.trieste.it

n° of text pages: 35

n° of tables: 4

n° of figures: 6

n° of references: 40

n° of words in the A*bstracts*: 193

n° of words in the *Introduction*: 561

n° of words in the *Discussion*: 992

JPET Fast Forward. Published on April 9, 2004 as DOI: 10.1124/jpet.104.066175
This article has not been copyedited and formatted. The final version may differ from this version.

ABSTRACT

The intra-tumor (i.t.) injection, of 35 mg/kg/day NAMI-A for 6 consecutive days, to CBA mice bearing i.m. implants of MCa mammary carcinoma reduces primary tumor growth and particularly lung metastasis formation, causing 60 % animals free of macroscopically detectable metastases. The i.t. treatment allows studying the effects of NAMI-A on *in vivo* tumor cells, exposed to mM concentrations for a relatively prolonged time. In these conditions, NAMI-A reduces the number of CD44+ tumor cells and changes tumor cell phenotype to a lower aggressive behaviour, as shown by SEM analysis. On primary tumor site, NAMI-A causes the unbalance between 2n and aneuploid cells in favor of lymphocytes. Furthermore, in tumor tissue, nitric oxide production is increased, active Mmp-9 decreased and these effects are accompanied by a reduced hemoglobin concentration.

These results are in agreement with the reduction of tumor invasion and metastasis and suggest the therapeutic usefulness of NAMI-A in neoadjuvant or tumor reduction treatments for preventing metastasis formation. These data further stress the usefulness of intratumor treatments as experimental preclinical model for studying *in vivo* the mechanism of tumor cell interactions after prolonged exposure to ruthenium-based compounds to be developed for metastasis inhibition.

JPET Fast Forward. Published on April 9, 2004 as DOI: 10.1124/jpet.104.066175
This article has not been copyedited and formatted. The final version may differ from this version.

INTRODUCTION

ImH[*trans*-$RuCl_4$(DMSO)Im] (Im= imidazole, DMSO= dimethylsulfoxide) (NAMI-A) is a metal-based compound effective against lungs metastases of solid tumors in murine models (Sava et al., 1998). This effect was always dissociated from a concomitant similar reduction of primary tumor growth and to any significant cytotoxic effect *in vitro* on human and on murine tumor cell lines up to mM concentrations (Bergamo et al., 2000; Pacor et al., 2001; Sava et al., 2003). These peculiarities make of NAMI-A an interesting compound for treating human disseminated tumors with a yet unknown mechanism of action, however different from that of "classical" cytotoxic chemotherapeutic drugs. Recently, NAMI-A has completed a phase I clinical trial at the Netherlands Cancer Institute of Amsterdam (The Netherlands) on 24 patients, without any unexpected toxicity and a MTD at doses compatible with those active on metastases in preclinical models (Schellens J.H.M., personal communication to Sava G.).

Chemical studies pointed out the propensity of NAMI-A to give hydrolyzed species in physiological conditions, but only the unmodified molecule is capable to bind to DNA (Bacac et al., 2004). In order to expose tumor cells to the unmodified molecule of NAMI-A, and to highlight the role of DNA as preferential target for the selective antimetastatic activity, we performed an i.t. treatment in a gel-carrier system, with the aim of achieving *in situ* a concentration higher and for prolonged times than that obtained with systemic routes.

Recently, local administration (intratumoral, i.t.) of drugs has lead to a proliferation of researches with the double aim of improving therapeutic outcomes and of limiting adverse systemic events (Goldberg et al., 2002). The great interest about i.t. drug administration is confirmed by the rising number of studies on animal models (Smith et al., 1999) and clinical trials (Vogl et al., 2002). The therapeutic target of such site-specific treatment was a large variety of inoperable advanced malignant solid tumors. The drugs utilized for these kinds of treatment are, usually, incorporated into carriers like purified bovine collagen gel matrix (Malhotra and Plosker, 2001), slow-release polymers (Jackson et al., 2000) or microspheres (Goldberg et al., 1994).

Besides information's on the efficacy of i.t. treatment against tumor growth and metastasis formation, the use of this route of administration will also help us to get more insight about the modality of action of this ruthenium compound that has always been given up today by systemic routes. More specifically, the aim of the study is that of analyzing the effects of NAMI-A on tumor cells and on tumor infiltrating lymphocytes (TIL) with particular attention to CD44 expression. CD44 family, an ubiquitous group of *trans*-membrane adhesion glycoproteins, is involved in cell-cell and cell-matrix interactions (Green et al., 1988; Lesley et al., 1993), lymphocyte homing and activation (Gal et al., 2003; DeGrendele et al., 1997), transmission of growth signals and others. The external protein's domain acts mainly as a hyaluronic acid (HA) binder, while the cytoplasmic domain is bound to ankyrin, a cortex protein involved in the regulation of cell cytoskeleton

(Bourguignon et al., 1995; Naot et al., 1997). Recent studies have demonstrated that CD44 is involved in the metastatic process at two crucial levels: cell adhesion to the extra-cellular matrix and cell motility (Herrera-Gayol and Jothy, 1999). Several studies have highlighted the possible use of CD44 expression level as a predictor/prognostic factor of metastatic potential (Xin et al., 2001; Yamaguchi et al., 2002; Wobus et al., 2002).

JPET Fast Forward. Published on April 9, 2004 as DOI: 10.1124/jpet.104.066175
This article has not been copyedited and formatted. The final version may differ from this version.

METHODS

Compound and treatment. Imidazolium *trans*-imidazoledimethylsulfoxide tetrachlororuthenate, ImH[*trans*-$RuCl_4$(DMSO)Im] (NAMI-A) (Figure 1), was prepared according to Mestroni (Mestroni et al., 1998). The compound was dissolved in a solution of 1:1 volume ratio of isotonic apyrogenic saline and Matrigel® 50µg/kg, in order to reach a final Matrigel® concentration of 25µg/kg. NAMI-A was administered intratumorally at the dose of 35 mg/kg/day at days 10^{th}-15^{th} from tumor implant, for overall 6 days of treatment. Control animals were treated in the same way with NAMI-A-free solution. We assumed that the subcutaneous tumor mass is physically identifiable with a solid derived from a rotation ellipsoid with a major and minor axis. Before treatment, the daily dose was divided into two aliquots of same volume that were administered on days 10, 12 and 14 at the two extremities of the major axis and on days 11, 13 and 15 at the two extremities of the minor axis after tumor implantation.

Tumor model. The murine mammary carcinoma (MCa) was utilized. Briefly, tumor line was locally maintained by serial bi-weekly passages of 10^6 viable tumor cells, obtained from donors similarly inoculated two weeks before, and injected i.m. into the calf of the left hind leg of CBA/Lac female adult mice (Poliak-Blazi et al., 1981). Tumor propagation for experimental purpose was performed by subcutaneous implant. Primary tumor measurement, metastasis count and mass evaluation. Primary tumor growth was quantified with caliper measurements, by determining two orthogonal axis and calculating tumor weight

with the formula: $(\pi/6)*\alpha^2*\beta$, being α the shorter and β the longer axis, considering d=1 . Tumor measures were taken every two days, on days 10^{th} - 22^{nd} from tumor implant. Metastases were counted and measured, with graduated ocular, at light microscope. The overall metastasis mass per mouse was calculated by applying the same formula used for the primary tumor to each single metastatic nodule. Number and mass of metastases were taken at day 22^{nd}. Animal studies. Animal studies were carried out according to the guidelines in force in Italy (DDL 116 of 21/2/1992 and subsequent addenda) and in compliance with the Guide for the Care and Use of Laboratory Animals, DHHS Pub. No (NIH) 86-23. Bethesda, MD: NIH, 1985.

Preparation of samples for atomic absorption spectroscopy. Lungs, liver, kidneys, primary tumor, blood (0,4-0,5 ml) and part of tail were taken 24 hrs and 168 hrs after last administration (respectively day 16^{th} and day 22^{nd} from tumor implant). A fragment of each tissue, and 50µl of plasma, obtained from an aliquot of blood, were put in crio-vial, carefully weighed, and stored for ruthenium (Ru) quantitation analysis by means of Atomic Absorption Spectroscopy (AAS). Samples were processed according to a modification of the procedures described by Tamura and Arai (1992). All specimens were dried in crio-vials. A first step of drying was performed overnight at 80°C, a second step at 105°C, until the samples reached the constant dried weight. The decomposition of the dried samples was carried out with the addiction of 100 µl of

tetramethylammoniumhydroxide (TMAH) at 25% in water (Aldrich Chimica, Italy) and 100 µl of milliQ directly in the vials. Volumes were adjusted to 0,5 ml with milliQ water. Ruthenium quantitation**.** The concentration of ruthenium in biological samples was measured in triplicate by means of Graphite Furnace Atomic Absorption Spectrometry (GFAAS), model SpectrAA-300, supplied with a specific ruthenium emission lamp (Hollow cathode lamp P/N 56-101447-00) Varian, Mulgrave, Victoria, Australia. Before each daily analysis session a five point calibration curve was traced using Ruthenium Custom-Grade Standard 998 mg ml^{-1}, Inorganic Ventures Inc. (Saint Louis, USA). In order to correct for possible deterioration of the graphite furnace during a daily working session, after every twelve samples the calibration curve was re-traced and a reslope standard was measured every six samples. The lower and higher limits of quantitation (LLQ, HLQ) were set at the concentration levels which corresponds respectively to the lowest and higher standard concentration employed. The limit of detection (LOD) was estimated according to: EURACHEM guide "The fitness for purpose of analytical methods". LLQ, HLQ and LOD were respectively: 20, 100 and about 10 ng*Ru*ml^{-1} of sample. The quantitation of ruthenium was carried out in 10 µl samples at 349.9 nm with an atomizing temperature of 2,500°C, using argon as purge gas at a flow rate of 3.0 l min^{-1}. For further details concerning the furnace parameter settings see Cocchietto et al. (Cocchietto and Sava, 2000).

Measurement of nitrite formation.

NO production was evaluated quantifying nitrite (NO_2^-) accumulation by a colorimetric assay according to the protocol of Steuhr and Nathan (1989). Aliquots of the samples were harvested from tumor suspension and allowed to react with nitrate reductase and $NADPH^+$ and then with an equal volume of Griess reagent (1% sulfanilamide in 5% phosphoric acid and 0,1% naphthylethylenediamine dihydrochloride in distilled water). The mixture was incubated in a flat –bottom 96-well culture plate for 10 min at room temperature. The absorbance was measured at 540 nm in a spectrophotometer. The values were obtained by comparison with standard concentrations of sodium nitrite.

MMP activity test

$2x10^6$ cells from the tumor homogenate were taken, frozen, thawed and determination of protein content was done according to Bradford procedure. Cells' samples were mixed with electrophoresis sample buffer [2% SDS, 10% glycerol, 50 mM Tris-HCl (pH 6.8) and 0.005 % bromophenol blue], sonicated and 80 µg of protein extracts were electrophoresed in 10% polyacrylamide-separating gel, in presence of 1% SDS and containing 1 mg/ml gelatin, without reducing or heating. Then gels were washed twice for 30 min with 2.5% Triton X-100 to remove SDS and finally washed three times for 5 min with distilled water. Gels were incubated overnight with collagenase buffer [50 mM Tris-HCl (pH 7.4), 200 mM NaCl and 5 mM $CaCl_2$]. They were stained for 4h in 30% methanol/10% glacial acetic acid containing 0.1% Coomassie Brilliant Blue R-250 and de-stained with the same solution without dye. Gelatinolitic activity was

JPET Fast Forward. Published on April 9, 2004 as DOI: 10.1124/jpet.104.066175
This article has not been copyedited and formatted. The final version may differ from this version.

detected as clear bands on the blue background. Molecular weight standard (6,500-205,00, SIGMA) was run on each gel. Densitometric analysis was done by Gel compare II software.

Hemoglobin quantitation

Hemoglobin was quantified in tumoral suspension and in blood using the Drabkin method (Drabkin and Austin, 1935) and Drabkin reagent kit 525 (Sigma, St Louis, MO, USA).

Flow cytometric analyses. DNA staining of primary tumor mass. $0.5x10^6$ cells of primary tumor mass, obtained as described above, were stained with PI (propidium iodide) ipotonic solution (0.5 mg PI /ml H_2O.) and left overnight before analysis. CD44/PI staining of lymphocytes and tumor cells after density gradient separation**.** Tumor cells, obtained after gradient separation on Hystopaque®, were stained with CD44-FITC and PI for a contemporaneous determination of cell membrane receptor and cell cycle. Briefly, $0.5x10^6$ cells were stained with CD44-FITC (2 μg, Southern Biotechnology Associates Inc., AL, USA), for 60 min, 4°C in the dark, and washed twice with PBS-NaN_3-BSA (phaosphate-buffered saline-sodium azide- albumin serum bovine). The cells were then fixed with 1% Paraformaldehyde, for 15 min, washed twice with PBS, permeabilised with methanol 100% (added on vortex) and left for further 15 min. Methanol was removed by washing the cells twice with PBS and twice with PBS-NaN_3-BSA-Saponin 0.1%. The last washing solution was maintained for 30 min.

JPET Fast Forward. Published on April 9, 2004 as DOI: 10.1124/jpet.104.066175
This article has not been copyedited and formatted. The final version may differ from this version.

The cells were then resuspended in 0.5 ml PBS containing 2.5 μg PI, RNase (4 μg/ml) and left overnight before analysis. All steps were performed at 4°C. Circulating lymphocyte typing by monoclonal antibodies. Circulating lymphocytes were obtained from blood harvested by cardiac puncture from anestethyzed animals. To avoid blood coagulation, 0.25 ml EDTA (0.1 M) was used. Briefly, 25 μl blood/animal was stained with fluorescent monoclonal antibodies (MoAb), CD3-FITC, CD19-PE (phycoerytreine), CD4-FITC and CD8-PE and CD44-FITC (all from Southern Biotechnology Associates Inc., Birmingham, AL, USA, SBA) for 30min, at 4°C, dark. Unbound antibodies were removed by washing twice with PBS-NaN_3-BSA. Blood samples were then treated with NH_4Cl solution, for 5 min at room temperature, to allow erythrocyte lysis. After washing with PBS-NaN_3-BSA, the cells were resuspended with PBS; all steps were performed at 4°C and analyzed by Flow Cytometry. Aliquots treated with an irrelevant isotype matched and FITC/PE MoAb, run in parallel, were used to set the gates in the monoparametric histogram to include less than 2% aspecific fluorescence events. All flow cytometric analyses were performed with the EPICS-XL2 instrument (Coulter Inst. Fl, USA). At least 10000 events were acquired for each sample. Histograms were analyzed with the WinMDI software (Dr. J. Trotter, Scripps Research Institute, La Jolla, CA, USA).

Scanning electron micrographs. Primary tumor mass, obtained as described above, was re-suspended in PBS ($20x10^6$ cell/ml). A drop of each cell suspension

was layered onto slides, previously coated with poly-L-lysine solution (0.1 mg/ml), and allowed to adhere for two hours at 4°C. Cells were then fixed with 2.5% glutaraldehyde, at 4°C, in 0.1 M cacodylate buffer overnight. Samples were then dehydrated in graded ethanol, vacuum dried and mounted onto aluminum scanning electron micrograph (SEM) mounts. After sputter coating with gold, they were submitted for analysis with the Leica Stereoscan 430i instrument, at the Electronic Microscopy Section, CSPA, University of Trieste, Italy.

Statistical analysis. Determinations of significant differences among groups were assessed by computerized program Instat graphpad; statistical tests employed are reported in each table.

JPET Fast Forward. Published on April 9, 2004 as DOI: 10.1124/jpet.104.066175
This article has not been copyedited and formatted. The final version may differ from this version.

RESULTS

Effects on primary tumor growth and on metastasis formation. The effects of i.t. administration of NAMI-A on primary tumor growth, measured from day 10 up to day 21 after tumor implantation, are showed, in Figure 2. The reduction of tumor mass is statistically significant vs controls ($p<0.05$) starting 24 hrs after the last i.t. administration (-36%); the highest reduction was measured on day 21 (-62%, $p<0.01$).

The effects on metastases are shown on Table 1. Metastasis number is reduced to about 1/3, and the whole metastatic mass undergoes a 6- to 7-times reduction vs controls while the lungs of 60% of treated animals were free of macroscopically detectable metastases.

Ruthenium quantitation. Ruthenium levels in tumor cell suspensions, lungs, kidney, liver, and plasma, after i.t. treatment, are listed in Table 2. Data represent concentrations of ruthenium measured respectively 24 hrs and 168 hrs after last NAMI-A administration. 24 hrs after the end of treatment, the higher ruthenium concentration was found in tumor cell suspensions; after further 6 days this value decreased by about one order of magnitude. Compared to intratumor concentration, decrease of NAMI-A from lungs is markedly slower, suggesting a stronger binding of this ruthenium compound in this tissue.

Diploid/aneuploid cell distribution inside tumor mass suspension. PI staining of tumor cell suspensions**,** obtained from the tumor mass of untreated and of treated animals shows a different percentage of 2n and of aneuploid cells (Figure

JPET Fast Forward. Published on April 9, 2004 as DOI: 10.1124/jpet.104.066175
This article has not been copyedited and formatted. The final version may differ from this version.

3, Panel A); quantitative data are reported in Figure 3, Panel B. The ratio of 2n vs. aneuploid cells is about 1:1 in untreated animals and 3:1 in the group of animals treated with NAMI-A.

Effects on hemoglobin levels, nitric oxide production and MMP activity. Hemoglobin quantification performed on peripheral blood and on tumor cell suspensions, at 24 and 168 hrs, and nitric oxide quantification performed at 168 hrs after the end of i.t. treatment are reported in Table 3. No appreciable difference of hemoglobin concentration between treated and untreated animals is found on peripheral blood samples; conversely, on tumor cell suspensions, a significant reduction ($p<0.05$) of hemoglobin levels between treated and untreated animals is observed 168 hrs after the end of treatment. At this time of observation, also a significant accumulation of nitrites in the samples of tumors of the treated mice is evidenced ($p<0.05$).

Gelatin zymography assays on primary tumor extracts, harvested 168 hrs after the end of treatment, are reported in Figure 4. Metalloprotease activity in samples of untreated controls (lane A) evidences a degradation band at 92kD, corresponding to gelatinase MMP-9, while no appreciable gelatinolitic activity at 72kD is detectable, compared to the reference positive control cell line HT1080 (lane C). NAMI-A (lane B) reduces the gelatinolitic activity (MMP-9) of the tumor extracts by about 56%, as results from densitometric analysis and as is reported in the lower Panel of Figure 4.

JPET Fast Forward. Published on April 9, 2004 as DOI: 10.1124/jpet.104.066175
This article has not been copyedited and formatted. The final version may differ from this version.

CD44 expression on leukocytes. The evaluation of CD44+ lymphocytes and of monocyte/polymorph-nucleated cells from peripheral blood of control and of NAMI-A-treated mice, detected by flow cytometry analysis following staining with appropriate MoAb at 24 and 168 hrs from the end of treatment, is shown in Table 4. NAMI-A increases the number of CD44+ lymphocytes by about 30% at any time of evaluation. No modifications of monocyte/polymorph-nucleated cells occur in the treated group as compared to untreated controls.

CD44 expression in aneuploid cells and in TIL. Flow cytometry analysis of CD44+ aneuploid and TIL cells, measured 24 and 168 hrs after last NAMI-A injection, are reported in Figure 5. At both 24 and 168 hrs, control samples (Panel A) show a weak percentage of CD44+ diploid cells and samples of NAMI-A treated mice (Panel B) do not significantly differ from controls. Conversely, control aneuploid cells show a relevant fraction of positive cells (above 35% of CD44+ over the total), a percentage that significantly drops in the NAMI-A treated group (Panel A). At 168 hrs, the percentage of CD44+ aneuploid cells of control animals rise to above 60%, while aneuploid cells in the treated animals remain low and comparable to those measured at 24 hrs.

SEM analysis. SEM analysis of tumor cell suspensions from untreated animals shows MCa tumor cells characterized by a convolute membrane, with “lamellipodia” and “phylopodia”, namely “invadopodia” (Figure 6, Panel A). This “aggressive” phenotype also correlates with the formation of homotypic aggregates (Panel B). Conversely, *ex vivo* cells from NAMI-A treated animals

display a simpler membrane (Panel C) and a significant interaction between leukocytes and tumor cells (Panel D).

JPET Fast Forward. Published on April 9, 2004 as DOI: 10.1124/jpet.104.066175
This article has not been copyedited and formatted. The final version may differ from this version.

DISCUSSION

The results of this study demonstrate that i.t. treatment, in the MCa mammary carcinoma model, reduces the number and weight of lung metastases in a way comparable if not superior to that obtained with the i.p. systemic administration for the same number of injections (Sava et al., 2003). This treatment is a suitable manner of maintaining longer exposure of tumor cells to non-hydrolyzed NAMI-A (Bacac et al., 2004).

Ruthenium concentration in host tissues, after i.t. treatment, is comparable to that obtained after systemic therapy, whereas in the primary tumor matrix, 24 hrs after last administration, it reaches a concentration of almost one order of magnitude higher than that in the other tissues analyzed. Six days later, intra-tumor ruthenium concentration drops to about one tenth, still maintaining a value above the maximum level observed after i.p. treatment (Sava et al., 2002). The persistence of a high amount of NAMI-A in the tumor is responsible for the progressive reduction of primary tumor mass, statistically significant from 24 hrs after treatment onward. This effect is consistent with the reported *in vitro* anti-proliferative threshold of NAMI-A on a number of tumor cell lines, which has been estimated to fall in the range of mM or grater concentrations (data on file). In the present work, this threshold is reached and maintained in the tumor mass for several days.

Nevertheless, this effect should not be simply attributed to cell cytotoxicity, since, also in this condition, as already reported in detail (Sava et al., 2003), NAMI-A results more active against cells endowed with metastatic ability as results from a consistent number of animals free of macroscopically detectable colonies.

The unbalance between 2n/aneuploid ratio, in the treated animals, indicates that tumor reduction is due to tumor cell reduction paralleled by a consistent increase of TIL. The pronounced effect of NAMI-A on lung metastases, greater than that reported in previous works (Cocchietto et al., 2003) may be ascribed to the greater effect on primary tumor growth with a more complete elimination of the clone of the tumor cells endowed with metastatic ability (Sava et al., 2003).

NAMI-A effect on tumor cells seem to be attributable to its ability to modulate malignancy parameters such as CD44 expression. It is known that the increase of CD44+ tumor cells is associated to an enhanced HA-binding which in turn is related to cell migration and invasiveness (Bourguignon et al., 1981; Bartolazzi et al., 1994; Zhang et al., 1995). In our experimental conditions, NAMI-A significantly reduces the percentage of CD44+ tumor cells, and this reduction is present up to seven days after the end of treatment.

Also “invadopodia”, i.e. cellular structures involved in tumor cell motility (Monsky et al., 1994; Mueller and Chen, 1991), are markedly reduced in tumor cells of the treated animals. Interestingly, these two markers show a close correlation, since CD44 is crucial to link the cortex protein ankyrin to the

membrane-associated actomyosin contractile system, required for the formation of “invadopodia” and for the consequent tumor cell migration (Bourguignon et al., 1981). Reduction of "invadopodia" in tumor cells may also explain the decreased gelatinolitic activity of primary tumor, since it has been reported that MMP-9, in its proteolytically active form, is preferentially localized inside “invadopodia” (Monsky et al., 1994; Mueller and Chen, 1991). Thus, NAMI-A down-regulates CD44, reduces the formation of “invadopodia” and down-modulates MMP-9 release, therefore interfering with the malignant properties of MCa tumor cells necessary to degrade the extracellular matrix and to allow tumor cell invasion and metastatic dissemination. These data are in agreement with the recent observations of the effects of NAMI-A on F-actin (Sava et al., 2004) and on α1-dependent contractile activity in aorta smooth muscle (Vadori M., PhD thesis data, Department of Biomedical Sciences, University of Trieste).

Another indication of modifications inside primary tumor, important for metastasis inhibition, is given by the significant lower levels of hemoglobin induced by local treatment with NAMI-A, as compared to untreated controls. These results are fully in agreement with the reported data of the effects of NAMI-A on EA.Hy926 (Vacca et al., 2002), ECV304 (Pintus et al., 2002, Sanna et al., 2002) endothelial cell lines, and in *in vivo* angiogenic systems (Vacca et al., 2002, Morbidelli et al., 2002). The overall data dealing with pronounced

antiangiogenic effects correlated to the reduction of MMPs release by cells inside primary tumor.

The appearance of numerous leukocytes into primary tumor mass and of CD44+ lymphocyte increase in the peripheral blood, seem to suggest a role for NAMI-A in promoting extravasation of blood lymphocytes throughout CD44 up-regulation. It is in fact known that CD44-HA interaction, a pathway that mediates primary adhesion, can address lymphocytes to specific extra-lymphoid effector sites (DeGrendele et al., 1997). Once arrived into the primary tumor, lymphocytes down-regulate CD44 but increase nitric oxide production, as shown by the significant accumulation of nitrites in tumor cell suspensions obtained *ex vivo* from treated animals; an early burst of production of nitric oxide (NO) is reported as a sign of lymphocyte activation (Beltran et al., 2002).

These data strongly suggest that the antimetastatic effects of NAMI-A depend on the reduction of the malignant phenotype of tumor cells and they are consistent with recent data indicating the stable and long-lasting effect of metastasis reduction for several transplant generations (Sava et al., 2003). This effect might be contributed by the potent action of NAMI-A on lymphocyte recruitment from circulation and to the consequent regulatory effects of these host cells on tumor growth and metastasis. NAMI-A i.t. administration seems thus an useful tool for neoadjuvant therapies, particularly where prognostic factors suggest high malignant tumors with elevated probability of metastatic dissemination.

Acknowledgements: Flow cytometry and Atomic Absorption Spectroscopy facilities were kindly provided by Fondazione C & D Callerio. The sample of NAMI-A used for experiment was kindly provided by E. Alessio, Department of Chemical Sciences, University of Trieste. The fellowship grants of Fondazione Callerio Onlus to the authors M.B., C.T., A.C. is gratefully acknowledged.

In memory of Maria Donata Gori.

REFERENCES

Bacac M, Hotze A, van der Schilden K, Pacor S, Alessio E, Haasnoot J, Sava G and Reedijk J (2004) NMR spectroscopy study of the coordination of the antimetastasis ruthenium complex [H2im]trans-Ru[RuCl4(dmso)(Him)], NAMI-A to DNA model bases, correlation of its chemical stability with biological activity assessed by flow cytometry. *J Inorg Biohem* 98: 402-412.

Bartolazzi A, Peach R, Aruffo A and Stamenkovic I (1994) Interaction between CD44 and Hyaluronate is directly implicated in the regulation of tumor development. *J Exp Med* 180: 53-66.

Beltran B, Quintero M, Garcia-Zaragoza E, O'Connor E, Esplugues JV and Moncada S (2002) Inhibition of mitochondrial respiration by endogenous nitric oxide: a critical step in Fas signaling. *PNAS* 99: 8892-8897.

Bergamo A, Zorzet S, Gava B, Sorc A, Alessio E, Iengo E and Sava G (2000) Effects of NAMI-A and some related ruthenium complexes on cell viability after short exposure of tumor cells. *Anti Cancer Drugs* 11: 665-672.

Bourguignon LY, Lida N, Welsh CF, Zhu D, Krongrad A and Pasquale D (1995) Involvement of CD44 and its variant isoforms in membrane-cytoskeleton interaction, cell adhesion and tumor metastasis. *J Neurooncol* 26: 201-208.

Bourguignon LYW, Zhu D and Zhu H (1981) CD44 isoform-cytoskeleton interaction in oncogenic signaling and tumor progression. *Frontiers in Bioscience* 3: 637-649.

Cocchietto M and Sava G (2000) Blood concentration and toxicity of the antimetastasis agent NAMI-A following repeated intravenous treatment in mice. *Pharmacol and Toxicol* 87: 193-197.

Cocchietto M, Zorzet S, Sorc A and Sava G (2003) Relationship between in vivo distribution of NAMI-A to primary tumour, lungs and kidney following different routes of administration and metastasis inhibition. *Invest New Drugs* 21: 1-8.

DeGrendele HC, Estess P and Siegelman MH (1997) Requirement for CD44 in activated T cell extravasation into an inflammatory site. *Science* 278: 672-675.

Drabkin DL and Austin JH (1935) Spectrophotometric studies. II. Preparations from washed blood cells; nitric oxide hemoglobin and sulfhemoglobin. *J Biol Chem* 112: 51.

Gal I, Lesley J, Ko W, Stoop R, Hyman R and Mikecz K (2003) Role of the extracellular and cytoplasmatic domains of CD44 in the rolling interaction of lymphoid cells with hyaluronan under physiologic flow. *J Biol Chem* 278: 11150-11158.

Goldberg EP, Hasdba AR, Almond BA and Marotta JS (2002) Intratumoral cancer chemotherapy and immunotherapy: opportunities for nonsystemic preoperative drug delivery. *J Pharm Pharmacol* 54: 159-180.

Goldberg EP, Quigg J, Sitren H, Hoffman E and Jayakrishnan A (1994) Microsphere drug carriers for targeted chemo-immunotherapy and for intracellular infections. *Proc Soc Biomaterials* 155.

Green SJ, Tarone G and Underhill CB (1988) Aggregation of macrophages and fibroblasts is inhibited by a monoclonal antibody to the hyaluronate receptor. *Exp Cell Res* 178:224-232.

Herrera-Gayol A and Jothy S (1999) Adhesion proteins in the biology of breast cancer: contribution of CD44. *Exp Mol Pathol* 66: 149-156.

Lesley J, Hyman R and Kincade PW (1993) CD44 and its interaction with extracellular matrix. *Adv Immunol* 151: 271-335.

Jackson JK, Gleave ME, Yago V, Beraldi E, Hunter WL and Burt HM (2000) The suppression of human prostate tumor growth in mice by the intratumoral injection of a slow-release polymeric paste formulation of paclitaxel. *Cancer Res* 60: 4146-4151.

Malhotra H and Plosker GL (2001) Cisplatin/epinephrine injectable gel. *Drugs Aging* 18: 787-793.

Mestroni G, Alessio E and Sava G. New salts of anionic complexes of Ru(III), as antimetastatic and antineoplastic agents, PCT. C 07F 15/00, A61K 31/28. WO 98/00431 08.01.98.

Monsky WL, Lin CY and Chen WT (1994) A potential marker protease of invasiveness, is localized on invadopodia of human malignant melanoma cells. *Cancer Res* 54: 5702-5710.

Morbidelli L, Donnini S, Filippi S, Messori L, Piccioli F, Orioli P, Sava G, Ziche M (2003) Antiangiogenic properties of selected ruthenium(III) complexes that are nitric oxide scavengers. *Br J Cancer*. 88:1484-91.

Mueller SC and Chen WT (1991) Cellular invasion into matrix beads: localization of beta 1 integrins and fibronectin to the invadopodia. *J Cell Sci* 99: 213-225.

Naot D, Sionov RV and Ish-Shalom D (1997) CD44: structure, function, and association with the malignant process. *Adv Cancer Res* 71: 241-319.

Pacor S, Vadori M, Vita F, Bacac M, Soranzo MR, Zabucchi G and Sava G (2001) Isolation of a murine metastatic cell linee and preliminary test of sensitivity to the anti-metastasis agent NAMI-A. *Anticancer Res* 21: 2523-2530.

Pintus G, Taddolini B, Posadino AM, Sanna B, Debidda M, Bernardini F, Sava G, Ventura C. Inhibition of the MEK/ERK signaling pathway by the novel antimetastatic agent NAMI-A down-regulates *c-myc* gene expression and endothelial cell proliferation (2002) *Eur J Biochem* 269: 5861-5870.

Poliak-Blazi M, Boranic M, Marzan B and Radacic MA (1981) A transplantable aplastic mammary carcinoma of CBA mice. *Vet Arh* 51: 99-107.

Sanna B, Debidda M, Pintus G, Tadolini B, Posadino AM, Bennardini F, Sava G and Ventura C (2002) The anti-metastatic agent imidazolium trans-imidazoledimethylsulfoxide-tetrachlororuthenate induces endothelial cell apoptosis by inhibiting the mitogen-activated protein kinase/extracellular signal-regulated kinase signaling pathway. *Arch Biochem Biophys* 403: 209-218.

Sava G, Bergamo A, Zorzet S, Gava B, Casarsa C, Cocchietto M, Furlani A, Scarcia V, Serli B, Iengo E, Alessio E and Mestroni G (2002) Influence of

chemical stability on the activity of the antimetastasis ruthenium compound NAMI-A. *Eur J Cancer* 38: 427-435.

Sava G, Capozzi I, Clerici K, Gagliardi R, Alessio E and Mestroni, G (1998) Pharmacological control of lung metastases of solid tumors by a novel ruthenium complex. *Clin Expl Metastasis* 16: 371-379.

Sava G, Frausin F, Cocchietto M, Vita F, Podda E, Spessotto P, Furlani A, Scarcia V, Zabucchi G.(2004) Actin-dependent tumor cell adhesion after short-term exposure to the antimetastasis ruthenium complex NAMI-A *Eur J Cancer* in press.

Sava G, Zorzet S, Turrin C, Vita F, Soranzio MR, Zabucchi G, Cocchietto M, Bergamo A, Di Giovine S, Pezzoni G, Sartor L and Garbisa S (2003) Dual action of NAMI-A in inhibition of solid tumor metastasis: selective targeting of metastatic cells and binding to collagen. *Clin Cancer Res* 9: 1898-1905.

Smith JP, Kanekal S, Patawaran MB, Chen JY, Jones RE, Orenberg EK and Yu NY (1999) Drug retention and distribution after intratumoral chemotherapy with fluorouracil/epinephrine injectable gel in human pancreatic cancer xenografts. *Cancer Chemother Pharmacol* 44: 267-274.

Steuhr DJ and Nathan CT (1989) Nitric oxide: a macrophage product responsible for cytostasis and respiratory inhibition in tumor target cells. J Exp Med 169: 1543-1555.

Tamura H and Arai T (1992) Determination of ruthenium in biological tissue by graphite furnace AAS after decomposition of the sample by tetramethylammonium hydroxide. *Bunseki KagaKu* 41: 13-17.

Vacca A, Bruno M, Boccarelli A, Coluccia M, Ribatti D, Bergamo A, Garbisa S, Sartor L and Sava G (2002) Inhibition of endothelial cell functions and of angiogenesis by the metastasis inhibitor NAMI-A. *Br J Cancer* 86: 993-998.

Vogl TJ, Engelmann K, Mack MG, Straub R, Zangos S, Eichler K, Hochmuth K and Orenberg E (2002) CT-guided intratumoral administration of cisplatin/epinephrine gel for treatment of malignant liver tumors. *Br J Cancer* 12: 524-529.

Wobus M, Rangwala R, Shein I, Hennigan R, Coila B, Lower EE, Yassin RS and Sherman LS (2002) CD44 associates with EGFR and erbB2 in metastatizing mammary carcinoma cells. *Appl Immunohistochem Mol Morphol* 10: 34-39.

Xin Y, Grace A, Gallagher MM, Curran BT, Leader MB and Kay EW (2001) CD44V6 in gastric carcinoma: a marker of tumor progression. *Appl Immunohistochem Mol Morphol* 9: 138-142.

Yamaguchi A, Goi T, Yu J, Hirono Y, Ishida M, Iida A, Kimura T, Takeuchi K, Katayama K and Hirose K (2002) Expression of CD44v6 in advanced gastric cancer and its relationship to hematogenous metastasis and long-term prognosis. *J Surg Oncol* 79: 230-235.

Zhang L, Underhill CB and Chen LP (1995) Hyaluronan on the surface of tumor cells is correlated with metastatic behaviour. *Cancer Res* 55: 428-433.

Footnotes

*Work supported by MIUR (prot.2001053898_004 "Pharmacological mechanisms of the antimetastatic activity of metal-based drugs) and in the framework of COST D200005/01 action.

Legends for figures

Figure 1. Molecular structure of the antimetastatic compound NAMI-A

Figure 2. Effects of intratumoral treatment on MCa mammary carcinoma primary tumor growth.

Groups of 15 female CBA mice, implanted s.c. with $1.2x10^6$ MCa cells on day 0, were intratumorally treated on days 10-15 with NAMI-A gel solution (35 mg/kg/die). Primary tumor growth was measured from day 10 to sacrifice (21 day). The data represent the mean±S.E.M.; S.E.M's bar are omitted for clearness. Means marked with the asterisk are statistically different from untreated controls. (*= $p<0.05$, **= $p<0.01$, ANOVA, Tuckey-Kramer post test).

Figure 3. Diploid/aneuploid cell distribution.

Samples of single cell suspensions obtained from s.c. tumor specimens 24h after the last treatment were stained with PI ipotonic solution and analyzed by flow cytometry. The reported percentages were elaborated by Multicycle software. Panel A shows a representative 3D plot (x axes: PI FL3 fluorescence; y axes: SSlog; z axes: events). Panel B mean values ±S.E.M. (n=5). *= $p<0.05$ values stastistically significant from control group, ANOVA, Student Newman Keuls post-test

Figure 4. Gel zymography of primary tumor extracts.

Representative samples from primary tumor of control group (line A), of NAMI-A i.t. treated group (line B) or from the reference HT1080 cell line (line C) as positive control, are showed in the upper panel. Lower panel: each histogram represent the mean value±S.E.M. (n=5) of the densitometric analysis performed.

Figure 5. Analysis of CD44+ cells in primary s.c. tumor i.t. treated.

Samples obtained from s.c. primary tumors were labelled with CD44 MoAb and cells were divided in aneuploid (tumour cells) and diploid (TIL), on the basis of different DNA content by contemporaneous PI staining. Histograms represent mean (n=8) ±S.E.M. of CD44 positive cells, analysed 24h (Panel A) or 168h (Panel B) after the last treatment at flow cytometer.

a= $p<0.05$, b= $p<0.001$ ANOVA, Student Newman Keuls post-test

Figure 6. SEM analysis of samples obtained from primary s.c. tumors.

Panel A and B are specimens from control group and panel C and D of NAMI-A i.t. treated mice.

JPET Fast Forward. Published on April 9, 2004 as DOI: 10.1124/jpet.104.066175
This article has not been copyedited and formatted. The final version may differ from this version.

Table 1. Effects of intratumoral treatment on pulmonary metastasis formation of MCa mammary.

	Metastases		
	Number	Weight (mg)	Met.-free
Control	30.8±5.6	136.8±36.5	0/15
NAMI-A	10.5±2.6*	20.8±4.4*	9/15

Each value is the mean of 15 samples ± S.E.M. (*= $p<0.05$ vs. control, unpaired t-test). Met-free: metastasis free animals. §= Frequencies are statistically different from each other ($p<0.05$, Fisher test).

JPET Fast Forward. Published on April 9, 2004 as DOI: 10.1124/jpet.104.066175
This article has not been copyedited and formatted. The final version may differ from this version.

Table 2. NAMI-A tissue uptake in murine model after a six-days-long intratumoral treatment

Time after last treatment (hrs)	Tissue	ng Ru/mg tissue
24	lungs	21.7±2.0
	liver	26.7±2.8
	kidneys	40.5±1.5
	tum. homog.	618.7±127.2
	plasma	8.0[a]±0.7
168	lungs	17.9±2.6
	liver	17.7±1.1
	kidneys	27.1±2.1
	tum. hom.	57.1±16.4
	plasma	0.6[a]±0.1

Tum. hom.= tumor homogenate. [a]: 1µl of plasma is considered to be approximately=1mg. Each value is the mean of the pool of data obtained from two distinct experiments ± S.E.M.

Table 3. Evaluation of hemoglobin in blood and tumor cell suspensions and nitric oxide in tumor cell suspensions after 24 and 168 hours the end of intratumoral treatment of MCa with NAMI-A 35 mg/kg/die for 6 days.

Time after last Treatment (hrs)	GROUPS	BLOOD	TUMORAL SUSPENSION	
		Haemoglobin g/(dL)	Hemoglobin g/(dL)	NO (O.D. 540 nm)
24	Controls	3.21±0.39	2.40±0.32	0.16±0.01
	Treated	3.96±0.23	2.97±0.27	0.18±0.01
168	Controls	3.98±0.27	5.24±0.70	0.19±0.01
	Treated	3.38±0.13	3.55±0.45*	0.27±0.02*

The data represent the mean±S.E.M. obtained from 5 animals. The means marked with the asterisk are statistically different from untreated controls (*= $p<0.05$, unpaired t-test).

JPET Fast Forward. Published on April 9, 2004 as DOI: 10.1124/jpet.104.066175
This article has not been copyedited and formatted. The final version may differ from this version.

Table 4. Analysis of CD44+ circulating leukocytes

	lymphocytes		**Monocytes/PMN**	
	% CD44+		% CD44+	
	24h	168h	24h	168h
Control	52.03±1.29	55.11±1.29	99.7±0.1	99.3±0.2
NAMI-A	68.50±1.40*	71.90±1.74*	98.8±0.6	97.7±1.1

Blood samples from tumor bearing mice were labelled with CD44-FITC MoAb and analysed by flow cytometry. In table are reported the mean values (n=5)±S.E.M. of CD44 positive cells gated on lymphocytes and monocytes/PMN. *= $p<0.05$ ANOVA, Student Newman Keuls test

JPET Fast Forward. Published on April 9, 2004 as DOI: 10.1124/jpet.104.066175
This article has not been copyedited and formatted. The final version may differ from this version.

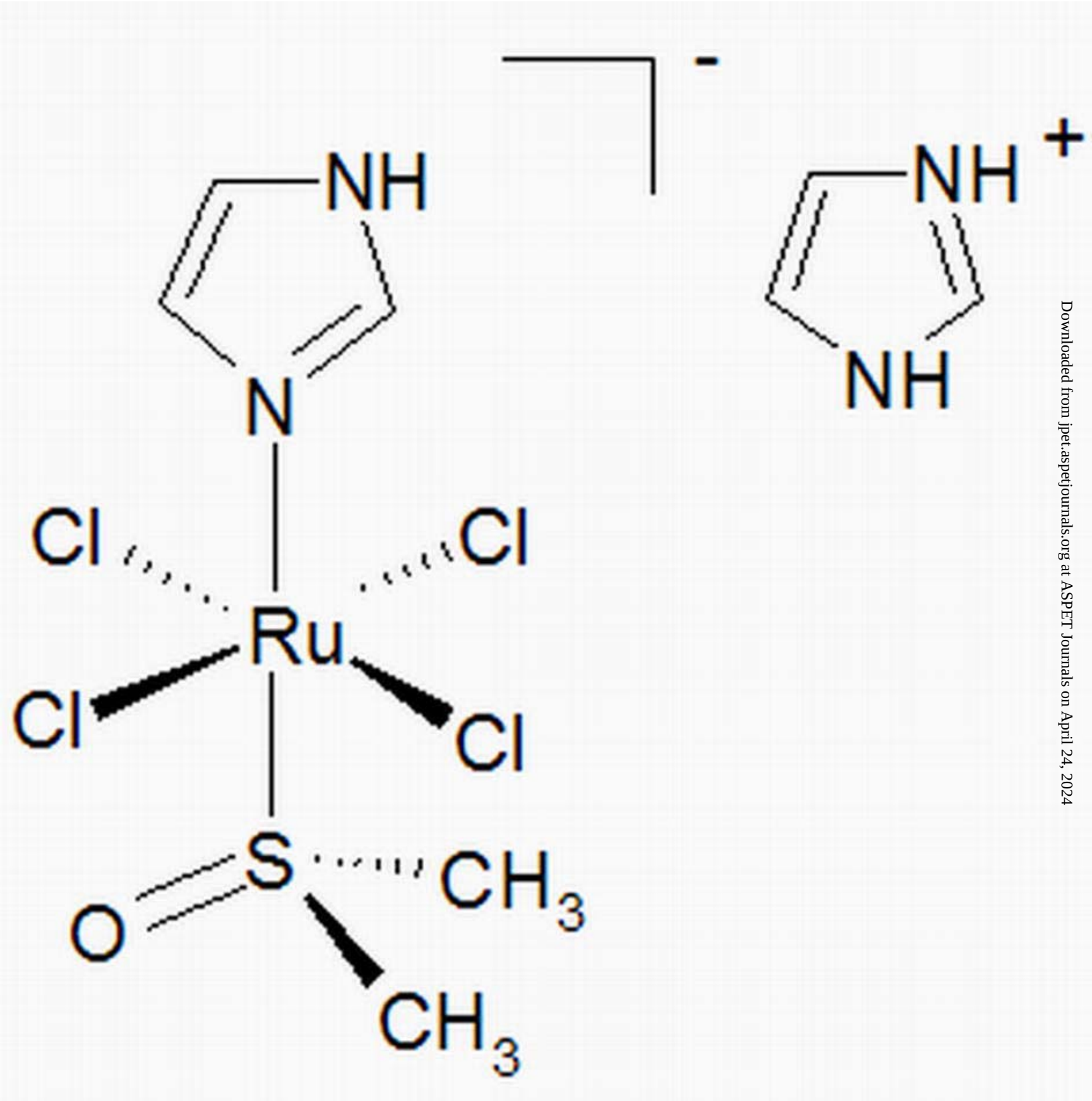

JPET Fast Forward. Published on April 9, 2004 as DOI: 10.1124/jpet.104.066175
This article has not been copyedited and formatted. The final version may differ from this version.

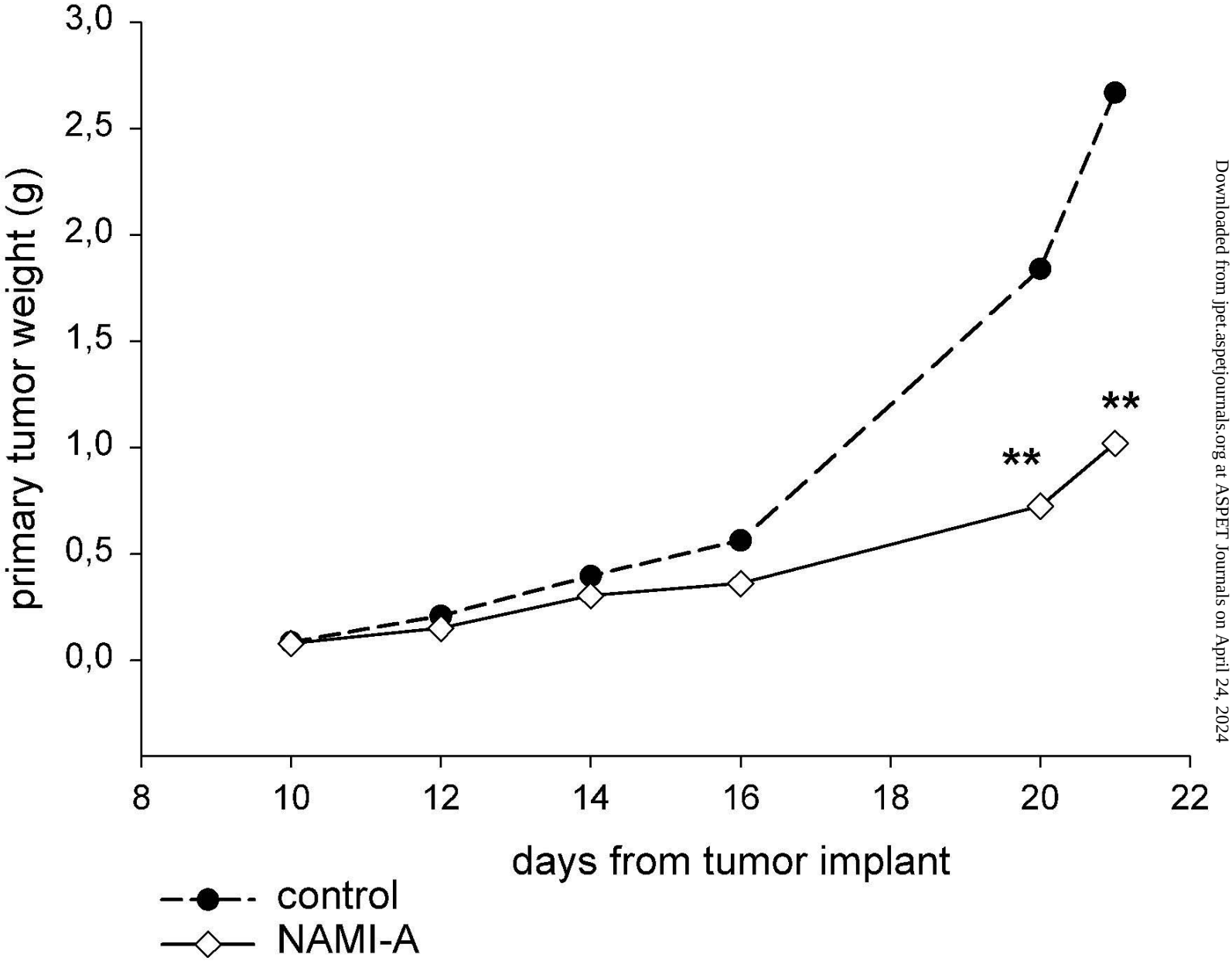

JPET Fast Forward. Published on April 9, 2004 as DOI: 10.1124/jpet.104.066175

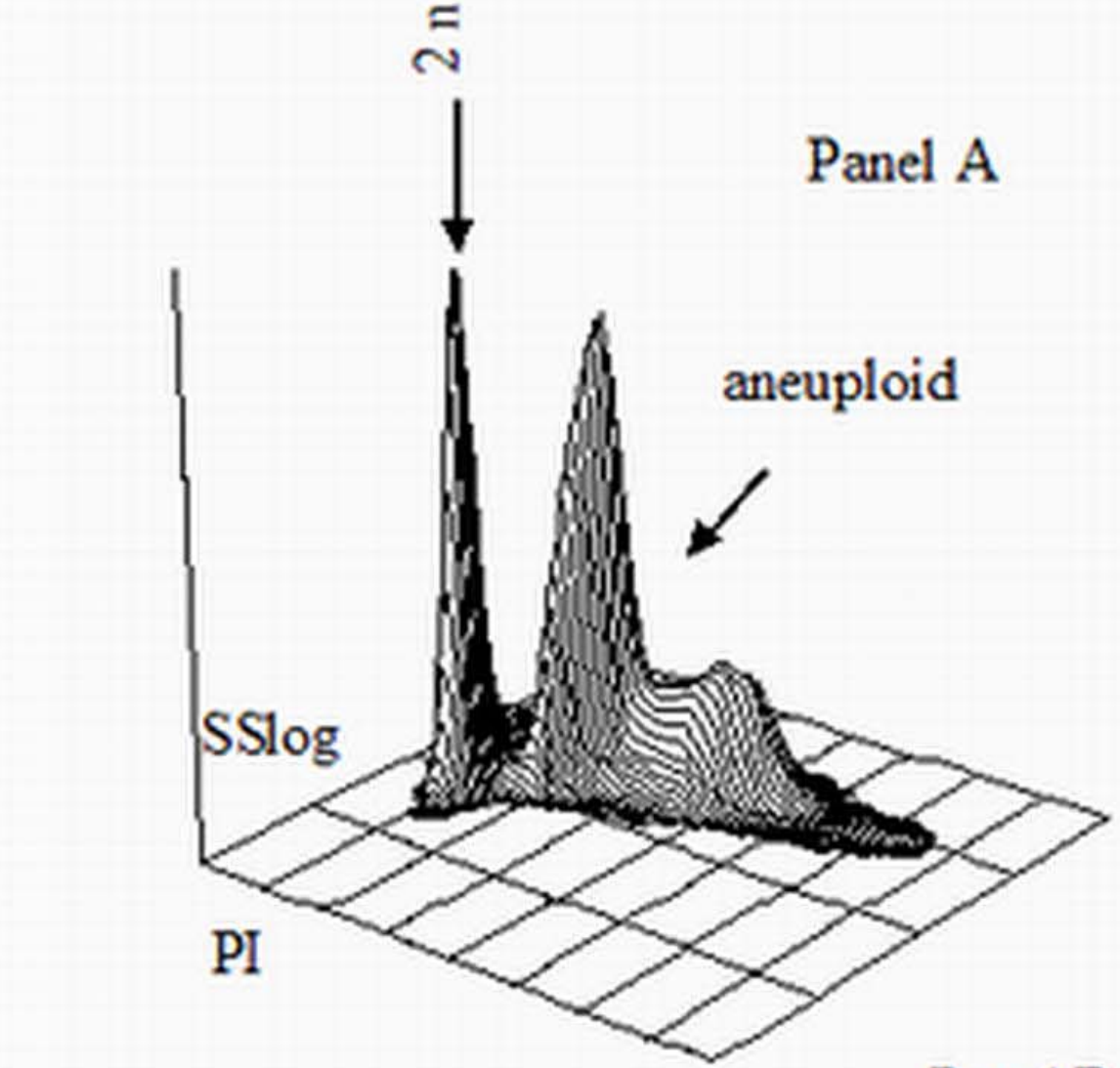

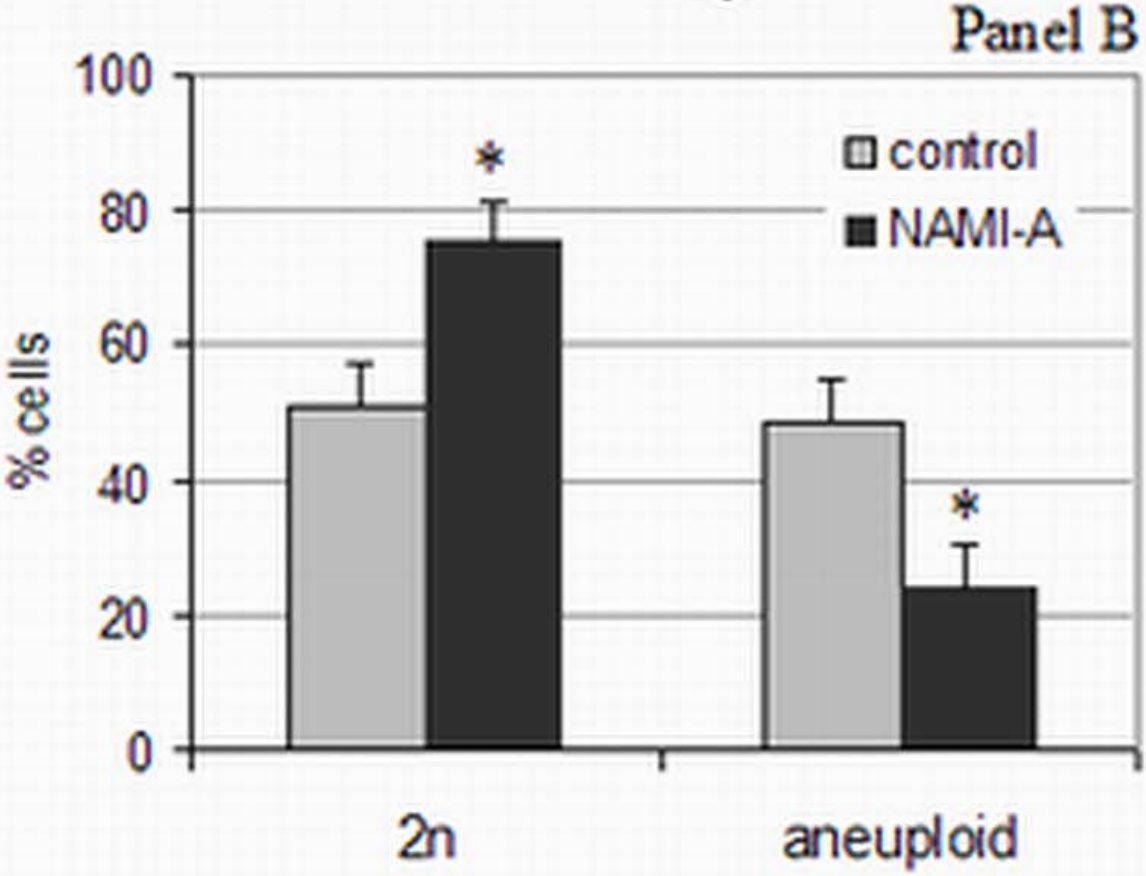

JPET Fast Forward. Published on April 9, 2004 as DOI: 10.1124/jpet.104.066175
This article has not been copyedited and formatted. The final version may differ from this version.

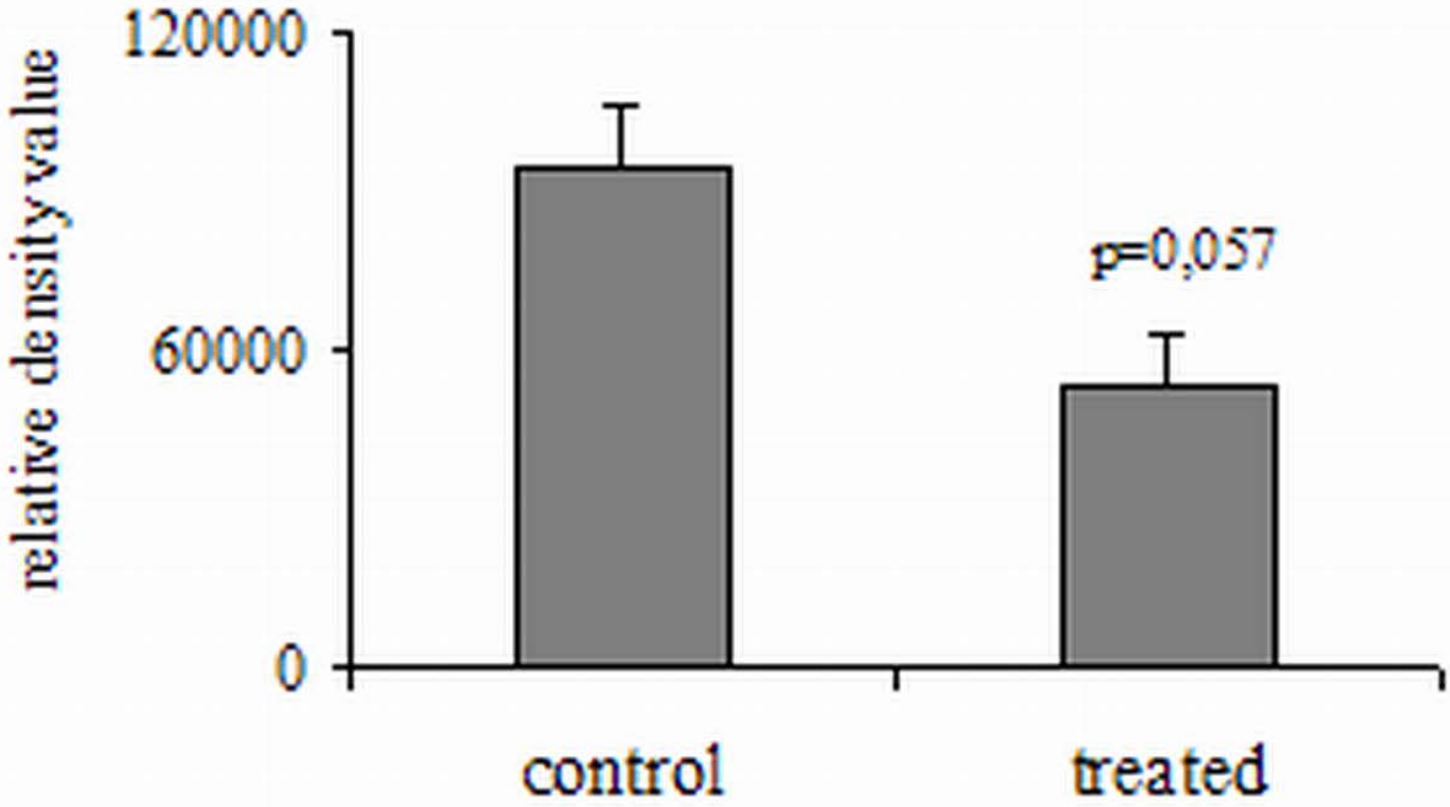

Panel A

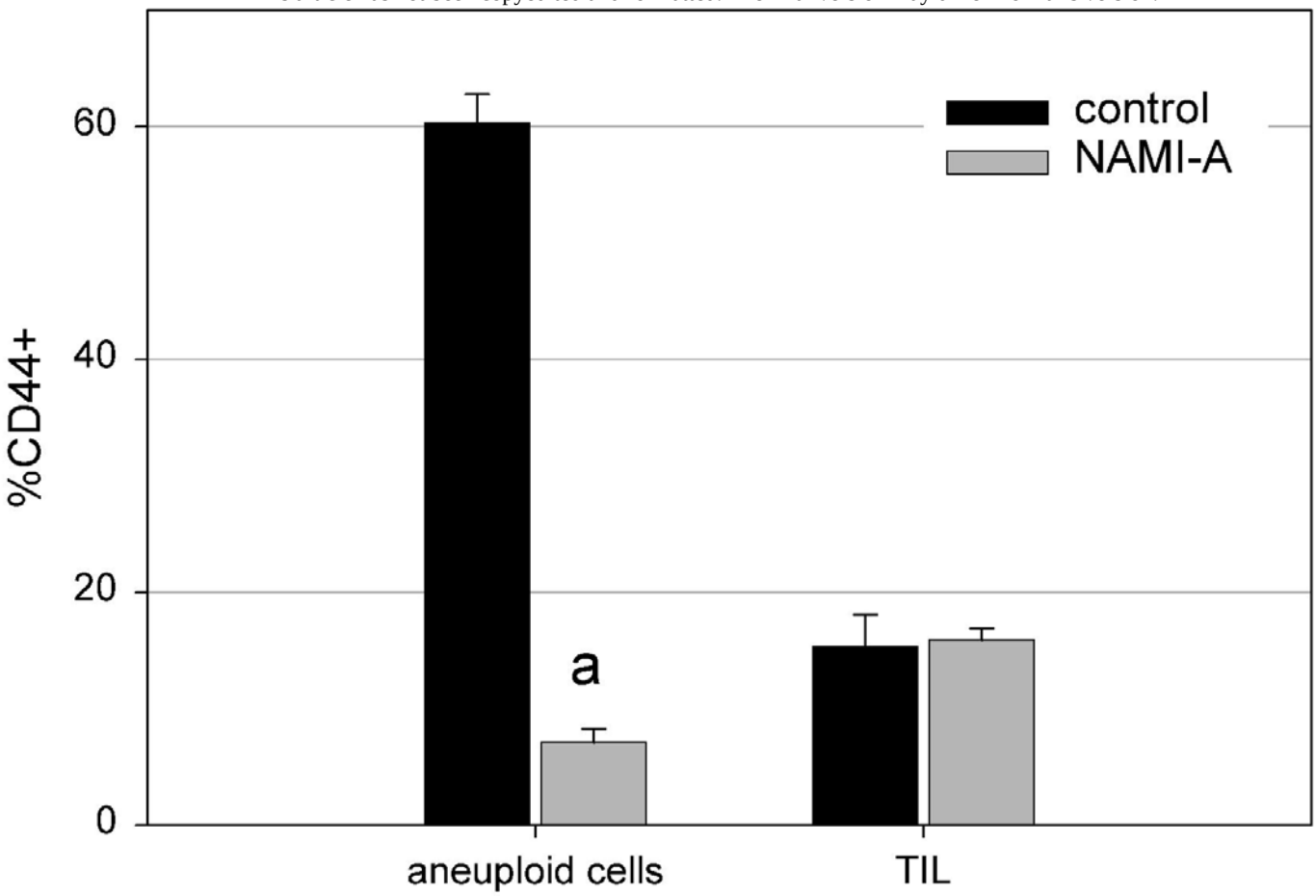

Panel B

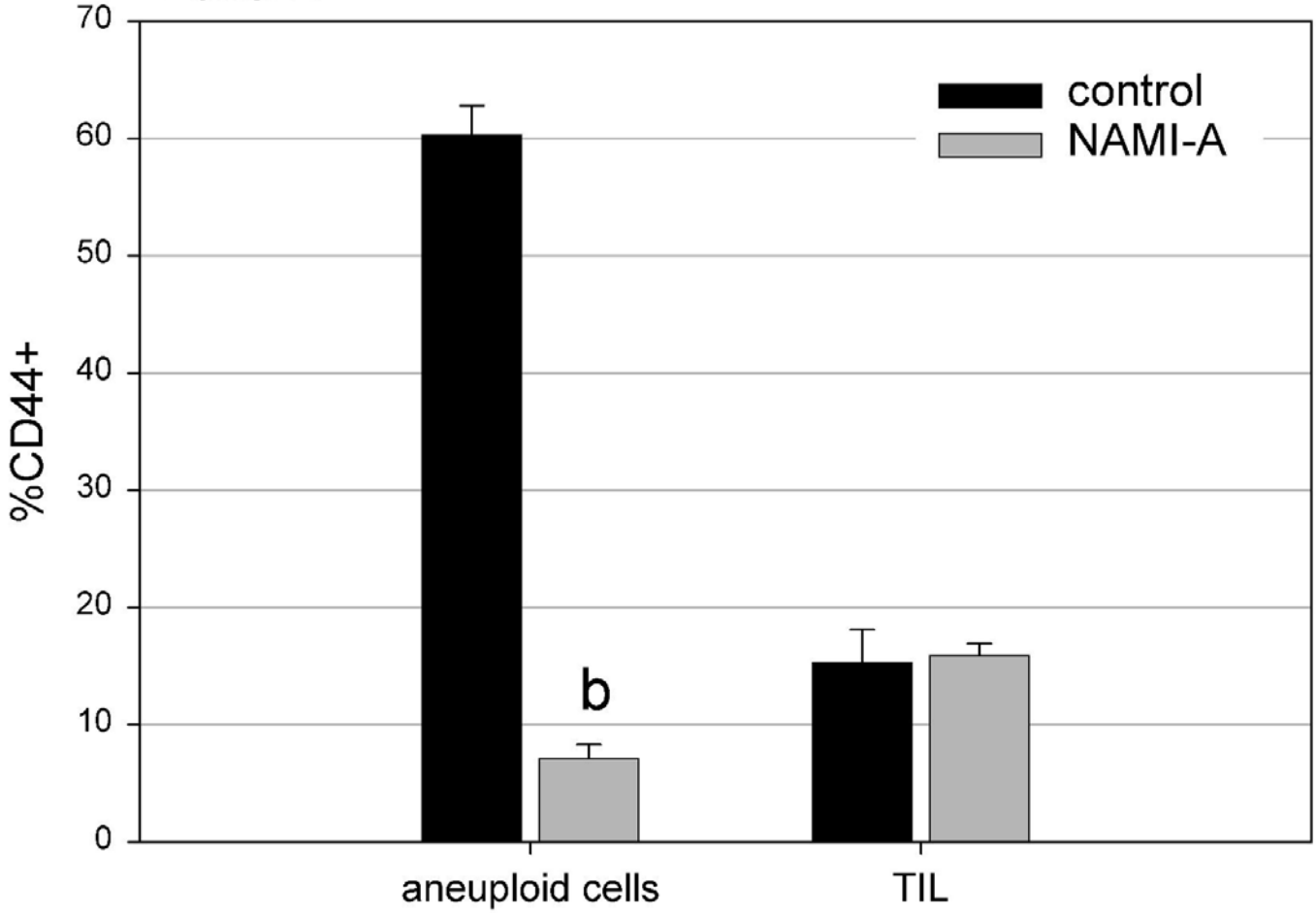

JPET Fast Forward. Published on April 9, 2004 as DOI: 10.1124/jpet.104.066175
This article has not been copyedited and formatted. The final version may differ from this version.